THE FASEB JOURNAL • RESEARCH • www.fasebj.org

Inhibition of human microsomal PGE2 synthase-1 reduces seizure-induced increases of P-glycoprotein expression and activity at the blood-brain barrier

Emma L. B. Soldner,[*] Anika M. S. Hartz,[†,‡] Shin-Ichi Akanuma,[§,¶] Anton Pekcec,[‖] Henri Doods,[‖] Richard J. Kryscio,[†,#] Ken-Ichi Hosoya,[¶] and Björn Bauer[§,,1]**

[*]Department of Pharmacy Practice and Pharmaceutical Sciences, College of Pharmacy, University of Minnesota, Duluth, Minnesota, USA; [†]Sanders-Brown Center on Aging, [‡]Department of Pharmacology and Nutritional Sciences, [§]Department of Pharmaceutical Sciences, College of Pharmacy, [#]Department of Statistics, and **Epilepsy Center, University of Kentucky, Lexington, Kentucky, USA; [¶]Department of Pharmaceutics, Graduate School of Medicine and Pharmaceutical Sciences, University of Toyama, Toyama, Japan; and [‖]Research Beyond Borders, Boehringer Ingelheim Pharma GmbH, Biberach an der Riss, Germany

ABSTRACT: The cause of antiseizure drug (ASD) resistance in epilepsy is poorly understood. Here, we focus on the transporter P-glycoprotein (P-gp) that is partly responsible for limited ASD brain uptake, which is thought to contribute to ASD resistance. We previously demonstrated that cyclooxygenase-2 (COX-2) and the prostaglandin E receptor, prostanoid E receptor subtype 1, are involved in seizure-mediated P-gp up-regulation. Thus, we hypothesized that inhibiting microsomal prostaglandin E_2 (PGE2) synthase-1 (mPGES-1), the enzyme generating PGE2, prevents blood-brain barrier P-gp up-regulation after status epilepticus (SE). To test our hypothesis, we exposed isolated brain capillaries to glutamate *ex vivo* and used a combined *in vivo–ex vivo* approach by isolating brain capillaries from humanized mPGES-1 mice to study P-gp levels. We demonstrate that glutamate signaling through the NMDA receptor, cytosolic phospholipase A2, COX-2, and mPGES-1 increases P-gp protein expression and transport activity levels. We show that mPGES-1 is expressed in human, rat, and mouse brain capillaries. We show that BI1029539, an mPGES-1 inhibitor, prevented up-regulation of P-gp expression and transport activity in capillaries exposed to glutamate and in capillaries from humanized mPGES-1 mice after SE. Our data provide key signaling steps underlying seizure-induced P-gp up-regulation and suggest that mPGES-1 inhibitors could potentially prevent P-gp up-regulation in epilepsy.—Soldner, E. L. B., Hartz, A. M. S., Akanuma, S.-I., Pekcec, A., Doods, H., Kryscio, R. J., Hosoya, K.-I., Bauer, B. Inhibition of human microsomal PGE2 synthase-1 reduces seizure-induced increases of P-glycoprotein expression and activity at the blood-brain barrier. FASEB J. 33, 000–000 (2019). www.fasebj.org

KEY WORDS: epilepsy · neurovasculature · ABCB1/MDR1

Over 70 million people worldwide suffer from epilepsy (1). Approximately 30–40% of patients have uncontrolled seizures because they are resistant to treatment with antiseizure drugs (ASDs) (1, 2). Thus, developing novel therapeutic strategies to effectively treat epilepsy is imperative.

One current research focus is on inflammation involved in the development and progression of CNS diseases. The prostanoid prostaglandin E_2 (PGE2) that is critical in the cyclooxygenase-2 (COX-2) inflammatory pathway is of particular interest. Under physiologic conditions, PGE2 is constitutively generated in the gastrointestinal tract, kidneys, vasculature, and bones (3, 4). Following seizures, however, brain PGE2 levels are substantially increased (5–7). Data from a recent study show that the cerebrovascular endothelium is the primary source of PGE2 during kainic acid–induced status epilepticus (SE) (6). PGE2 is thought to exert proconvulsive effects by enhancing neural hyperexcitability, increasing neuronal death, and impairing blood-brain barrier function (6, 8–11). In addition, PGE2 has been linked to seizure-induced up-regulation of the blood-brain barrier drug efflux transporter, P-glycoprotein (P-gp), that is known to transport ASDs (12–14). P-gp is up-regulated following seizures, especially in limbic brain regions commonly associated with seizure generation

ABBREVIATIONS: AA, arachidonic acid; ASD, antiseizure drug; BSA, bovine serum albumin; COX-2, cyclooxygenase-2; $cPLA_2$, cytosolic phospholipase A2; DPBS, Dulbecco's PBS; EP1, prostanoid E receptor subtype 1; ES, embryonic stem; hmPGES-1, human mPGES-1; mPGES-1, microsomal PGE2 synthase-1; NBD-CSA, *N*-ε(4-nitrobenzofurazan-7-yl)-D-Lys8–cyclosporin A; P-gp, P-glycoprotein; PGE2, prostaglandin E_2; PGF2-α, prostaglandin F2-α; PGH2, prostaglandin endoperoxide H_2; PGI2, prostacyclin; *PTGES*, prostaglandin E synthase gene; RRID, Research Resource Identifier; SE, status epilepticus; UK-ADC, Alzheimer's Disease Core Center–University of Kentucky

[1] Correspondence: Department of Pharmaceutical Sciences, College of Pharmacy, University of Kentucky, 333 Sanders-Brown Center on Aging, 800 S Limestone, Lexington, KY 40536-0230, USA. E-mail: bjoern.bauer@uky.edu

doi: 10.1096/fj.201901460RR

(9, 11, 12, 15–20). Moreover, P-gp up-regulation has been associated with ASD resistance (21, 22). Selective COX-2 inhibition in animal SE and epilepsy models reduced both PGE2 and P-gp expression, which increased ASD distribution and pharmacosensitivity (11, 20, 21). We have shown that inhibiting the PGE2 receptor, prostanoid E receptor subtype 1 (EP1), also prevents P-gp up-regulation following SE (9). Although COX-2 inhibitors are effective in preventing P-gp induction and improving pharmacosensitivity *in vivo* (21), they also have negative cardiovascular side effects. We, therefore, investigated the effect of inhibiting PGE2 production on P-gp after SE. The final step of PGE2 production is mediated by prostaglandin E synthase. In the brain, inducible microsomal prostaglandin E synthase-1 (mPGES-1) has been shown to be responsible for the increase in PGE2 after seizures (6). Thus, we hypothesized that inhibiting mPGES-1 prevents the induction of P-gp expression and transport function following SE.

Although 2 inhibitors of human mPGES-1 (hmPGES-1) have entered clinical trials, no mPGES-1 inhibitor is clinically available yet. Here, we report that BI1029539, a specific hmPGES-1 inhibitor, prevents seizure-induced P-gp up-regulation at the blood-brain barrier in transgenic mice expressing hmPGES-1. Based on our findings, we conclude that mPGES-1 is involved in the signaling pathway leading to seizure-induced up-regulation of efflux transporters and that mPGES-1 inhibition may potentially serve as a target to overcome ASD resistance in epilepsy that is mediated in part by P-gp. Furthermore, inhibiting hmPGES-1 with BI1029539 may also prove beneficial in treating other CNS diseases that involve PGE2 (23).

TABLE 1. *Western blot analysis of P-gp protein expression levels in isolated brain capillaries exposed to PGH2 and PGE2*

Exposure	P-gp
PGH2	
Control	100 ± 2.5
10 nM PGH2	183.7 ± 5.1*
25 nm PGH2	157.1 ± 4.6*
PGE2	
Control	100 ± 3.3
0.5 nM PGE2	132.1 ± 4.7*
0.75 nm PGE2	164.2 ± 5.7*
1 nm PGE2	193.4 ± 6.9*

Data were normalized to β-actin levels; values are given as percentage of control ± SEM ($n = 3$). See Fig. 2*A*, *C*. *$P < 0.01$ for each endpoint compared with control (Dunnett's many-to-one *t* test).

MATERIALS AND METHODS

Data and statistical analysis

Data and statistical analyses follow published guidelines for experimental design and analysis (24). Sample sizes (*e.g.*, animal numbers, number of brain capillaries to be analyzed) for individual experiments were based on power analyses of preliminary data and previously published data and are provided in the figure legends (12, 25). The number of repetitions is stated in the Results section and the figure legends. Animals were randomly assigned to each group (simple randomization); data analysis was performed in a blinded fashion.

Statistical analyses focused on comparisons among experimental groups and did not include covariates. Mean response was compared using a 2-tailed, unpaired Student's *t* test for 2 groups and ANOVA for more than 2 groups. Analyses were performed using Microsoft Excel (Microsoft, Redmond, WA, USA) and Prism [v.7.00; Research Resource Identifier (RRID): SCR_002798; GraphPad Software, La Jolla, CA, USA]. Because animals in each experiment were independent, observed differences were considered to be statistically significant when $P < 0.05$ (*i.e.*, there were no multiple comparisons based on data from the same animals). For the Western blot data in **Tables 1–5**, the mean for each treatment was compared with control using Dunnett's many-to-one *t* test with statistical significance determined at $P < 0.05$.

Chemicals

BI1029539 (alternative name: OX-MPI) was provided by Boehringer Ingelheim Pharma (Biberach, Germany) (26, 27). Antibody against hmPGES-1 (MBS240155) for immunohistochemistry was from MyBioSource (San Diego, CA, USA). hmPGES-1 (Clone6C6) antibody for Western blotting and immunostaining was from Cayman Chemical (Ann Arbor, MI, USA; 10004350, RRID: AB_10079051). Guinea pig–derived anti–mPGES-1 pAb was kindly provided by Ken-Ichi Hosoya (Toyama University, Toyama, Japan) (28–30). Kainic acid and β-actin antibody (ab8226) were obtained from Abcam (Cambridge, MA, USA). *N*-ε(4-nitrobenzofurazan-7-yl)-D-Lys8–cyclosporin A (NBD-CSA) was custom-synthesized by R. Wenger (Basel, Switzerland) (31). L-Glutamate, bovine serum albumin (BSA), glutaraldehyde (25%), and paraformaldehyde were purchased from MilliporeSigma (Burlington, MA, USA). Antibody against P-gp (C219; MA126528; RRID: AB_795165), Dulbecco's PBS (DPBS), DAPI, and all other chemicals and supplies were purchased from Thermo Fisher Scientific (Waltham, MA, USA).

Animals

Animal protocols were approved by the University of Minnesota Institutional Animal Care and Use Committee (1012A93932; Principal Investigator: B.B.) and were in accordance with Association for Assessment and Accreditation of Laboratory Animal Care (AAALAC) regulations, the U.S. Department of Agriculture Animal Welfare Act, U.S. National Institutes of Health animal guidelines, and the Animal Research: Reporting of *In Vivo* Experiments (ARRIVE) guidelines. Animals were housed under controlled conditions (24–26°C, 50–60% relative humidity, 12-h dark/light cycle) with free access to tap water and rodent chow. Prior to experimentation, animals were allowed to acclimate for 2 wk. For *ex vivo* experiments, male CD IGS Sprague-Dawley rats (RGD_734476; 8 wk of age, 275–300 g; Charles River Laboratories, Wilmington, MA, USA), male C57BL/6NTac mice (RRID: IMSR_TAC:b6; 8 wk of age, 20–23 g; Taconic Farms, Germantown, NY, USA), and male transgenic humanized mPGES-1 mice on a C57BL/6 background (8 wk of age, 20–23 g; Boehringer Ingelheim Pharma) were used. For *in vivo* studies, we used male and female C57BL/6NTac wild-type mice (11–14 wk of age, 20–30 g; Taconic Farms) as well as male and female transgenic humanized mPGES-1 C57BL/6 mice (12–14 wk of age, 20–34 g; Boehringer Ingelheim Pharma).

Generation of transgenic humanized mPGES-1 C57BL/6 mice

Transgenic mice constitutively expressing the mPGES1 [prostaglandin E synthase gene (*Ptges*)] humanized allele were generated by Boehringer Ingelheim Pharma using a similar strategy as previously reported in ref. 32. The mouse mPGES1 (*Ptges*)

TABLE 2. *Western blot analysis of P-gp protein expression levels in isolated brain capillaries exposed to glutamate, NMDA, AA, PGH2, and PGE2*

Exposure	P-gp
Glutamate	
Control	100 ± 4.3
100 μM glutamate	181 ± 5.7*
+1 μM SC51089	113.2 ± 5.5**
NMDA	
Control	100 ± 5.5
1 μM NMDA	174.5 ± 9.3*
+1 μM SC51089	113.0 ± 6.7
AA	
Control	100 ± 3.0
10 μM AA	192.5 ± 7.1*
+1 μM SC51089	107.9 ± 3.5
PGH2	
Control	100 ± 4.9
10 nM PGH2	182.4 ± 9.0*
+1 μM SC51089	105.8 ± 5.3
PGE2	
Control	100 ± 4.1
0.5 nM PGE2	190 ± 8.4*
+1 μM SC51089	132.5 ± 5.3*

Data were normalized to β-actin levels; values are given as the percentage of control ± SEM ($n = 3$). See Fig. 3. *$P < 0.01$, **$P < 0.05$ for each endpoint compared with control (Dunnett's many-to-one *t* test).

genomic region encompassing exon 1 (starting at the translation initiation site), intron 1, and exon 2 were replaced with an engineered human mini-gene (full-length human *PTGES* cDNA was engineered by inserting human *PTGES* intron 1 between exons 1 and 2). An additional polyadenylation signal was inserted downstream of exon 3, which contains the 3′ UTR, to improve the expression of the human *PTGES* cDNA in mouse cells and prevent downstream transcription of the remaining mouse gene. Mouse genomic sequences downstream of exon 2 were left intact in order to keep all potential regulatory elements driving expression of the mPGES1 (*Ptges*) gene. A positive selection marker (PuroR) was flanked by F3 recombination sites and inserted downstream of the human *PTGES* mini-gene. A targeting vector was generated using bacterial artificial chromosome clones from the C57BL/6J RPCI-23 bacterial artificial chromosome library and transfected into the TaconicArtemis C57BL/6N Tac embryonic stem (ES) cell line. Homologous recombinant clones were isolated using positive (puromycin resistance) and negative (thymidine kinase) selections, and the humanized allele was finalized after Flp-mediated removal of the selection marker. hmPGES-1 protein was expressed under the control of the endogenous mouse mPGES1 (*Ptges*) promoter. Because of the removal of mouse mPGES1 (*Ptges*) exons 1 and 2 and the termination of transcription at the inserted 3′UTR and polyadenylation signals within the human mini-gene, mouse mPGES-1 protein was no longer expressed. The C57BL/6N ES cell line was grown on a mitotically inactivated feeder layer composed of mouse embryonic fibroblasts in DMEM high-glucose medium containing 20% FBS (PAN-Biotech, Aidenbach, Germany) and 1200 U/ml leukemia inhibitory factor (Esgro Recombinant Mouse LIF Protein, ESG1107; MilliporeSigma). Cells (10^7) and 30 μg of linearized DNA vector were electroporated (Gene Pulser Xcell Electroporation System; Bio-Rad, Hercules, CA, USA) at 240 V and 500 μF. Puromycin selection (1 μg/ml) started on d 2 after electroporation; counterselection with gancyclovir (2 μM) started on d 5 after electroporation. ES clones were isolated on d 8 and analyzed by Southern blotting after expansion and freezing of clones in liquid nitrogen. After administration of hormones, superovulated BALB/c female mice were mated with BALB/c male mice. Blastocysts were isolated at 3.5 d postcoitum. For microinjection, blastocysts were placed in a drop of DMEM with 15% fetal calf serum under mineral oil. A flat-tip, piezo-actuated microinjection pipette with an internal diameter of 12–15 μm was used to inject 10–15 targeted C57BL/6NTac ES cells into each blastocyst. After recovery, 8 injected blastocysts were transferred to each uterine horn of pseudopregnant nuclear MRI (NMRI) female mice at 2.5 d postcoitum. Chimerism was measured in chimeras (G_0) by coat color contribution of ES cells to the BALB/c host (black and white). Highly chimeric mice were bred to strain C57BL/6 females. Germline transmission was identified by the presence of black, strain C57BL/6 offspring (G_1). Mice were backcrossed to the C57BL/6 background strain over at least 6 generations.

Human brain samples

Human brain samples (inferior parietal lobule, $n = 2$) were obtained from the brain bank of the Alzheimer's Disease Core Center at the University of Kentucky (UK-ADC; Lexington, KY, USA; Institutional Review Board B15-2602-M). Inclusion criteria included enrollment in the UK-ADC longitudinal autopsy cohort study, postmortem intervals ≤4 h, and final consensus diagnosis of normal cognition as determined by UK-ADC neuropathologists, neuropsychologists, and neurologists (33).

BI1029539 dosing and kainic acid–induced SE

BI1029539 (10, 30, 100 mg/kg) or vehicle (10% Tween 80; MilliporeSigma) and 90% Natrosol 250 HX (dosing volume: 10 ml/kg; Boehringer Ingelheim Pharma) were administered twice a day *via* oral gavage over 5 d (**Fig. 1**). Mice received 4 doses of BI1029539 or vehicle by oral gavage prior to inducing SE. After SE, mice received additional 3 applications of BI1029539 or vehicle.

SE was induced in both wild-type and transgenic hmPGES-1 mice by fractionated administration of kainic acid dissolved in isotonic saline (pH 7.4; control mice received saline instead of kainic acid). Specifically, mice were given an initial kainic acid bolus dose of 20 mg/kg, i.p. Mice that did not develop SE within 60 min of the initial bolus dose received additional kainic acid doses of 5 or 10 mg/kg, i.p. every 30 min until mice developed continuous seizure activity (SE). Subsequent doses of kainic acid were determined by the severity and frequency of seizures according to a protocol adapted from Hellier and Dudek (34). A subset of mice ($n = 12$, 2 male and 10 female mice) did not develop SE after kainic acid dosing and were kept as kainic acid controls. Mean cumulative kainic acid doses given were 33.7 ± 6.5 mg/kg for control

TABLE 3. *Western blot analysis of P-gp and hmPGES-1 protein expression levels in isolated brain capillaries exposed to glutamate and BI1029539*

Exposure	P-gp	hmPGES-1
Control	100 ± 7.0	100 ± 1.9
100 μM glutamate	166 ± 10.9*	132.8 ± 3.5*
+1 μM BI1029539	91.8 ± 6.7	91.5 ± 2.3*
1 μM BI1029539	91.0 ± 5.2	91.8 ± 1.7*

Data were normalized to β-actin levels; values are given as the percentage of control ± SEM ($n = 3$). See Fig. 5*C*. *$P < 0.01$ for each endpoint compared with control (Dunnett's many-to-one *t* test).

TABLE 4. *Western blot analysis of P-gp and hmPGES-1 protein expression levels in isolated brain capillaries exposed to glutamate and BI1029539*

Exposure	P-gp	hmPGES-1
Control	100 ± 4.8	100 ± 3.1
100 μM glutamate	174.9 ± 6.6*	149.5 ± 5.5*
1 nM BI1029539	103.3 ± 5.7	131.4 ± 4.7*
10 nM BI1029539	103.9 ± 5.1	97.4 ± 2.3
100 nM BI1029539	100.2 ± 5.3	100.2 ± 3.4

Data were normalized to β-actin levels; values are given as the percentage of control ± SEM ($n = 3$). See Fig. 6*A*. *$P < 0.01$ for each endpoint compared with control (Dunnett's many-to-one t test).

mice (no BI1029539) that experienced SE and 30.8 ± 0.4 mg/kg kainic acid for control mice (no BI1029539) that did not develop SE. Mean cumulative kainic acid doses given to mice that also received BI1029539 were 35.0 ± 6.2 mg/kg (10 mg/kg BI1029539), 43.6 ± 7.8 mg/kg (30 mg/kg BI1029539), and 33.9 ± 4.2 mg/kg (100 mg/kg BI1029539). Each group mean was compared with kainic acid control animals (no SE) using Satterthwaite's ~2-sample Student's t test because the variance of the responses in the control group was significantly less than the variance for any other group. To guard against inflation of the type I error rate, statistical significance was determined at the $P < 0.0125$ level (Bonferroni's correction). The SE group had a significantly smaller mean than control, and the 30 mg/kg BI1029539 group had a significantly larger mean than the control. The means for 10 mg/kg BI1029539 and 100 mg/kg BI1029539 did not differ from the control mean.

After 90 min, SE was terminated with repeated doses of 10 mg/kg, i.p. diazepam until seizures stopped (mean cumulative diazepam dose: 17.0 mg/kg). For post-SE recovery, mice were given 5% dextrose solution (3 ml, s.c.); supplemental heat was provided throughout recovery until mice were able to move, groom, and take in food and water. Mice were given Napa nectar (Systems Engineering, Napa, CA, USA) and critical care food (Oxbow Animal Health, Omaha, NE, USA) mixed with 5% dextrose until CO_2 euthanasia 48 h after SE. Control mice also received diazepam.

Brain capillary isolation

Brain capillaries were freshly isolated as previously described in refs. 35 and 36. Briefly, animals were euthanized by CO_2 inhalation and decapitated; brains were harvested and collected in ice-cold DPBS containing Ca^{2+} and Mg^{2+}, 5 mM D-glucose, and 1 mM sodium pyruvate, pH 7.4. Brain tissue was homogenized, mixed with Ficoll PM 400 (final concentration 15%; MilliporeSigma), and centrifuged (5800 *g*, 20 min, 4°C). The resulting capillary pellet was suspended in 1% BSA-DPBS and passed over a glass-bead column, from which capillaries were collected in 1% BSA-DPBS and washed with DPBS. For *ex vivo* glutamate experiments, capillaries were exposed to 100 μM glutamate for 30 min, washed, and incubated in glutamate-free buffer for 5.5 h. After a total of 6 h, brain capillaries were used for transport experiments, immunohistochemistry, and crude membrane isolations followed by Western blotting.

Western blotting

Freshly isolated brain capillaries were homogenized in CelLytic M lysis buffer (MilliporeSigma) containing Complete protease inhibitor (Roche, Basel, Switzerland). Samples were centrifuged (10,000 *g*, 15 min, 4°C) to remove cellular debris and nuclei. Further centrifugation (100,000 *g*, 90 min, 4°C) yielded a pellet of crude capillary membranes that was resuspended in tissue lysis buffer containing protease inhibitor and kept at −80°C until further use. Prior to Western blotting, sample protein concentrations were determined by Bradford assay. Western blotting was performed using the NuPage Bis-Tris Electrophoresis and blotting system (Thermo Fisher Scientific). Samples were mixed with 4× lithium dodecyl sulfate sample buffer and 10% DTT reducing agent. Samples were run in 4–12% Bis-Tris gradient gels and transferred for 1 h. Membranes were blocked for 1 h and incubated overnight at 4°C with primary antibody against β-actin (1:1000, 1 μg/ml, RRID: AB_306371; ab8226, Abcam), hmPGES-1 (3 μg/ml, RRID: AB_10079051; 10004350, Cayman Chemical), polyclonal rat-mouse mPGES-1 (0.1 μg/ml), or P-gp (C219, 1:100, 0.5 μg/ml, MA126528, RRID: AB_795165; Thermo Fisher Scientific) (30). Membranes were washed and incubated with horseradish peroxidase–conjugated ImmunoPure secondary IgG (1:10,000; Pierce, Rockford, IL, USA) for 1 h at room temperature. Protein bands were visualized using SuperSignal West Pico and West Femto chemiluminescent substrates (Pierce) and a ChemiDoc XRS imager (Bio-Rad). Optical density of protein bands was measured with Bio-Rad Quantity One software (v.4.6.9; Bio-Rad).

Immunohistochemistry

Immunohistochemistry of mouse brain capillaries was performed as described in Bauer *et al*. (37). Freshly isolated mouse brain capillaries were transferred onto #1 glass coverslips in imaging chambers and fixed for 30 min in 3% paraformaldehyde–0.25% glutaraldehyde at room temperature. Capillaries were washed with PBS, permeabilized for 30 min with 1% Surfact-Amps X-100 (Pierce), washed with PBS, and blocked with 1% BSA-PBS. Capillaries were incubated with primary monoclonal antibody against hmPGES-1 (1:100; 10 μg/ml in BSA, RRID: AB_10079051; 10004350, Cayman Chemical) or primary pAb against mPGES-1 (2 μg/ml; overnight at 4°C) (30). Capillaries were washed with 1% BSA-PBS and incubated with secondary antibody (1:1000 in BSA-PBS, 2 μg/ml; Pierce) for 1 h at 37°C in the dark. Nuclei were counterstained with DAPI (1 μg/μl in 1% BSA-PBS, 10 min). To control for background fluorescence, capillaries used as negative control were processed without primary antibody. Immunofluorescence was visualized with a Zeiss LSM 710 inverted confocal microscope that was equipped with a C-Apochromat ×40/1.2 W Corr objective using the 488 nm line of an argon laser (Carl Zeiss, Oberkochen, Germany).

TABLE 5. *Western blot analysis of P-gp and hmPGES-1 protein expression levels in isolated brain capillaries from animals that experienced SE that were treated with BI1029539 or vehicle*

Exposure	P-gp	hmPGES-1
Control	100 ± 5.0	100 ± 4.1
100 mg/kg BI1029539	98.7 ± 5.0	108.4 ± 4.3
Kainic acid control	139.0 ± 6.9*	92.9 ± 3.7
SE	190.5 ± 9.4*	146.9 ± 4.8*
SE + 10 mg/kg BI1029539	97.4 ± 4.1	95.6 ± 3.7
SE + 30 mg/kg BI1029539	107.3 ± 4.8	95.1 ± 3.9
SE + 100 mg/kg BI1029539	103.8 ± 5.3	95.5 ± 3.6

Data were normalized to β-actin levels; values are given as the percentage of control ± SEM ($n = 3$). See Fig. 7*A*. *$P < 0.01$ for each endpoint compared with control (Dunnett's many-to-one t test).

Ex vivo P-gp transport assay

P-gp transport activity in mouse brain capillaries was assessed using the fluorescent P-gp substrate NBD-CSA as described in refs. 35 and 38. Freshly isolated capillaries were transferred into imaging chambers and incubated with NBD-CSA (2 μM) for 1 h at room temperature. For each group, images of 10 capillaries were acquired with a Zeiss LSM 710 inverted confocal microscope (C-Apochromat ×40/1.2 W Corr objective, 488 nm line of an argon laser; Carl Zeiss). Luminal NBD-CSA fluorescence intensity was quantitated using Zeiss Zen 2012 Imaging software (Carl Zeiss). Specific, luminal NBD-CSA fluorescence was taken as the difference between total luminal fluorescence and fluorescence in the presence of the P-gp–specific inhibitor PSC833 (5 μM) (38–40).

RESULTS

Prostaglandin endoperoxide H_2 and PGE2 up-regulate P-gp in brain capillaries

We previously showed COX-2 involvement in glutamate-mediated up-regulation of P-gp at the blood-brain barrier (9, 12, 20). COX-2 is a proinflammatory enzyme that converts arachidonic acid (AA) to prostaglandin endoperoxide H_2 (PGH2), which is converted by mPGES-1 to PGE2 (41).

We exposed isolated rat brain capillaries to 0, 10, and 25 nM PGH2 for 6 h and observed increased P-gp protein expression levels in membranes from brain capillaries that were exposed to PGH2 compared with control capillaries (**Fig. 2*A***; Western blot analyses in Table 1). We also determined P-gp transport activity levels in isolated brain capillaries by using an assay we previously established (12, 25). In this assay, brain capillaries are incubated with the fluorescent P-gp substrate NBD-CSA (2 μM) for 1 h to steady state. Capillaries are imaged with a confocal microscope followed by quantitative image analysis of NBD-CSA fluorescence in the capillary lumen. In brain capillaries with high P-gp transport activity, more NBD-CSA is transported into the capillary lumen compared with control capillaries, resulting in higher luminal NBD-CSA fluorescence. Thus, luminal NBD-CSA fluorescence levels are a measure for P-gp transport activity. We utilized this assay to assess P-gp transport activity levels in brain capillaries exposed to PGH2. Consistent with increased P-gp protein expression, we found that nanomolar concentrations of PGH2 also increased P-gp transport activity in isolated rat brain capillaries (Fig. 2*B*). A similar effect was observed with PGE2, the product of mPGES-1–mediated conversion of PGH2. PGE2 is found at low nanomolar concentrations in the brain that typically are in the range of 0.02–10 nM (42–44). We found that 0.5, 0.75, and 1 nM PGE2 increased P-gp protein expression and transport activity (Fig. 2*C, D*). We further demonstrated that the mPGES-1 inhibitor BI1029539 prevents PGH2-mediated up-regulation of P-gp protein expression and transport activity (Fig. 2*E, F*).

Together, these findings suggest that PGH2, mPGES-1, and PGE2 are involved in the signaling pathway responsible for up-regulation of P-gp protein expression and transport activity levels at the blood-brain barrier.

PGE2 receptor 1 is involved in P-gp up-regulation in brain capillaries

Prostaglandins such as PGE2 exert their effects by signaling through prostaglandin receptors. We recently detected protein expression of the prostaglandin receptor EP1 in isolated rat brain capillaries and linked it to seizure-induced increase of P-gp protein expression and transport activity levels at the blood-brain barrier (9, 20). We previously also demonstrated that the neurotransmitter glutamate, which is extensively released during seizures, up-regulates P-gp expression and activity levels in isolated brain capillaries (12). Here, we show that blocking EP1 with the EP1 antagonist SC-51089 prevents glutamate-mediated up-regulation of P-gp protein expression and transport activity in isolated rat brain capillaries (**Fig. 3*A***). P-gp up-regulation was also observed in capillaries that were exposed to the NMDA receptor agonist NMDA; this effect was also abolished by blocking the EP1 receptor (Fig. 3*B*). We further found that the cytosolic phospholipase A2 ($cPLA_2$) product AA, the COX-2 product PGH2, and the mPGES-1 product PGE2 all up-regulate P-gp protein expression and transport activity levels (Fig. 3*C–E*) and that blocking EP1 with SC-51089 prevents these effects (Western blot analyses in Table 2).

These data suggest that AA, PGH2, PGE2, mPGES-1, and EP-1 are involved in the signaling pathway through which glutamate mediates P-gp up-regulation at the blood-brain barrier.

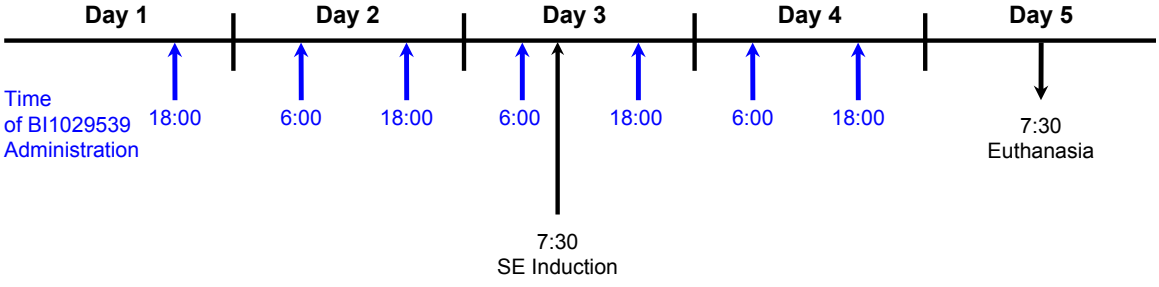

Figure 1. BI1029539 dosing regimen. BI1029539 (10, 30, 100 mg/kg) or vehicle was administered twice a day *via* oral gavage over a period of 5 d. Mice received 4 doses of either BI1029539 or vehicle by oral gavage prior to inducing SE in mice and additional 3 applications of either BI1029539 or vehicle after SE induction. Acute SE was induced in both wild-type and transgenic hmPGES-1 mice by fractionated administration of kainic acid.

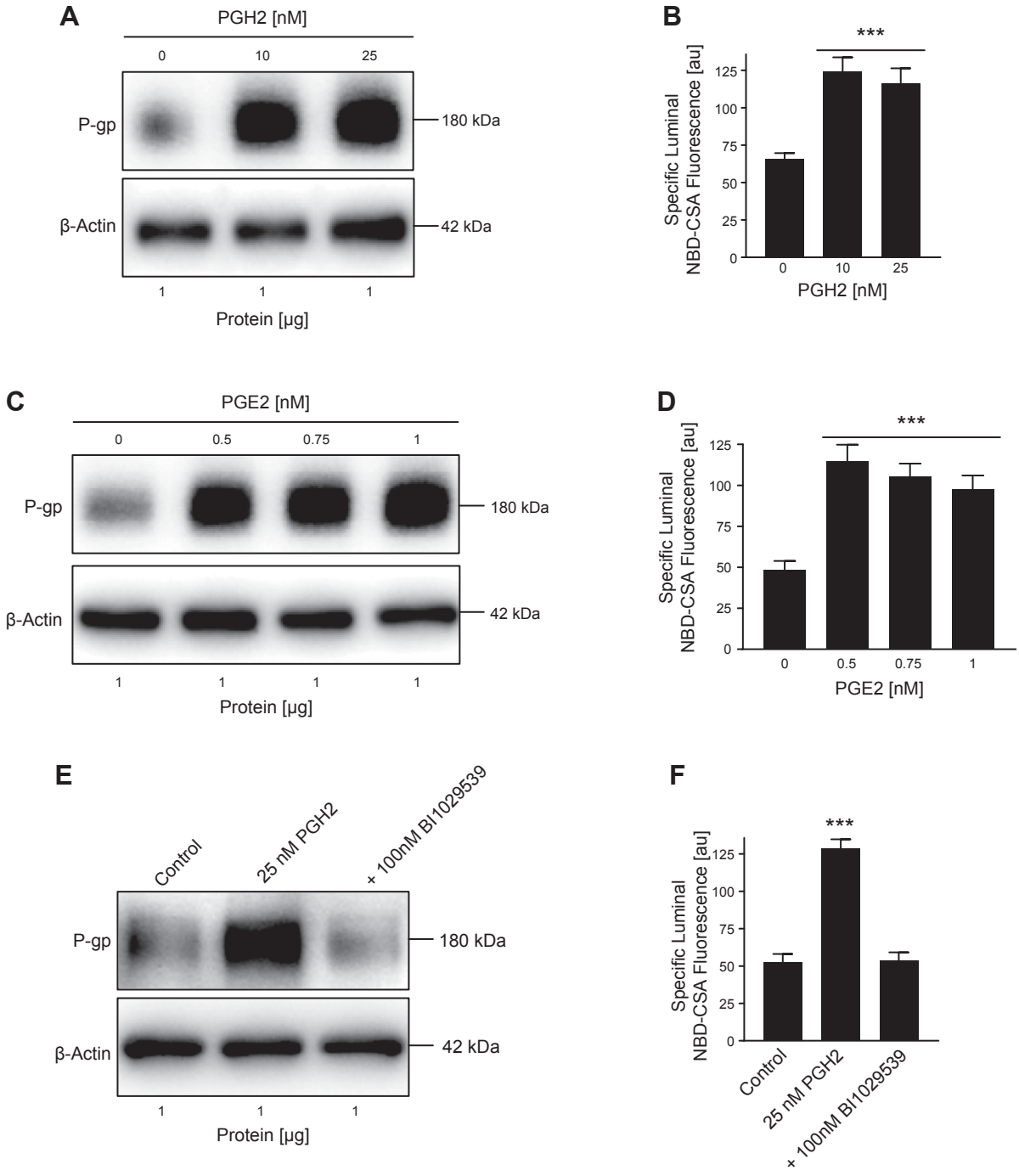

Figure 2. PGH2 and PGE2 up-regulate P-gp protein and activity levels in isolated brain capillaries. *A*) Western blot showing P-gp protein expression in isolated rat brain capillaries exposed to PGH2; β-actin was used as protein loading control. *B*) P-gp transport activity in isolated rat brain capillaries exposed to PGH2. *C*) Western blot showing P-gp protein expression in isolated rat brain capillaries exposed to PGE2; β-actin was used as protein loading control. *D*) P-gp transport activity in isolated rat brain capillaries exposed to PGE2. *E*, *F*) Exposing brain capillaries to 25 nM PGH2 increased P-gp protein expression and transport activity levels. This effect on P-gp was blocked by 100 nM BI1029539. For specific luminal NBD-CSA fluorescence, data represent means ± SEM for 10 capillaries from a single preparation (pooled tissue from 10 rats). Units are arbitrary units (au; scale: 0–255). ***$P < 0.001$, significantly higher than controls.

mPGES-1 expression in mouse, rat, and human brain capillaries

mPGES-1 is a major source of PGE2 by converting PGH2 into PGE2. Previous studies have demonstrated that mPGES-1 is constitutively expressed throughout the brain, including the area postrema, the subfornical organ, the paraventricular hypothalamic nucleus, the arcuate nucleus, the preoptic area, and the choroid plexus (29). On a cellular level, high expression of

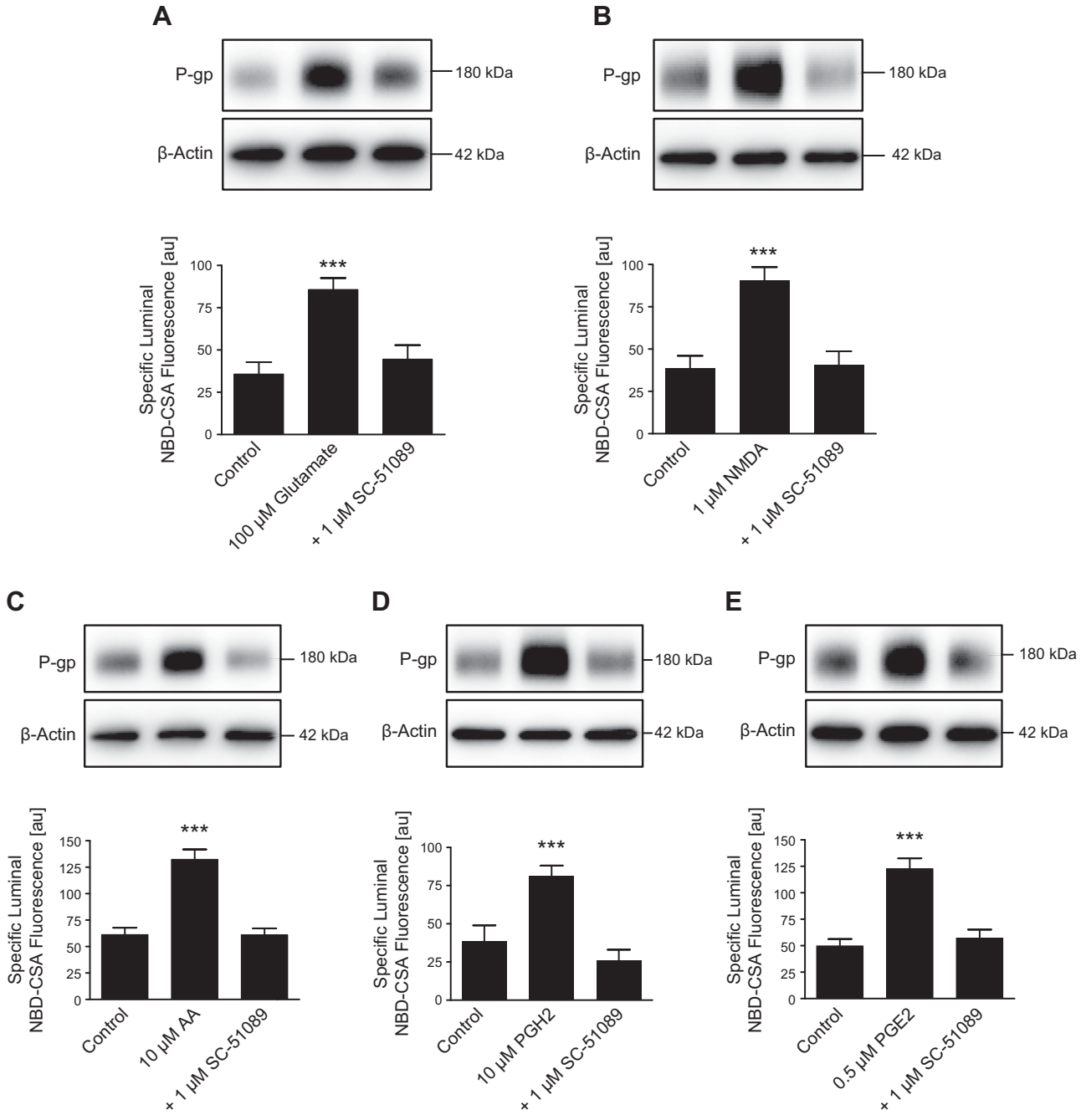

Figure 3. Glutamate increases P-gp protein and activity levels by signaling through the prostaglandin E receptor EP1. Isolated rat brain capillaries were exposed to glutamate (*A*), NMDA (*B*), AA (*C*), prostaglandin H2 (PGH2) (*D*), and PGE2 (*E*) with or without the EP1 inhibitor SC-51089. Blocking the EP1 receptor with SC-51089 fully abolished the action of glutamate, NMDA, AA, PGH2, and PGE2. P-gp protein expression was assessed by Western blotting; β-actin was used as protein loading control. P-gp transport activity was measured as specific luminal NBD-CSA accumulation in capillary lumens. For specific luminal NBD-CSA fluorescence, data represent means ± SEM for 10 capillaries from a single preparation (pooled tissue from 10 rats). Units are arbitrary units (au; scale: 0–255). ***$P < 0.001$, significantly higher than controls.

mPGES-1 has been shown in leptomeninges, astrocytes, capillary-associated pericytes, and brain endothelial cells comprising the blood-brain barrier. **Figure 4** shows representative images of immunostained mPGES-1 in brain capillaries isolated from human (Fig. 4*A*), rat (Fig. 4*B*), and mouse (Fig. 4*C*) brain tissue. Localization of mPGES-1 appears to be intracellular and in the luminal and abluminal membranes, which is consistent with mPGES-1 being an intracellular, membrane-associated protein (45). Western blot analysis of isolated capillary membranes from human, rat, and mouse brain capillaries suggests that mPGES-1 is highly expressed in mouse and human brain capillaries and to a lesser extent in isolated rat brain capillaries (Fig. 4*D*). Together, our data demonstrate mPGES-1 expression at the blood-brain barrier of mouse, rat, and human.

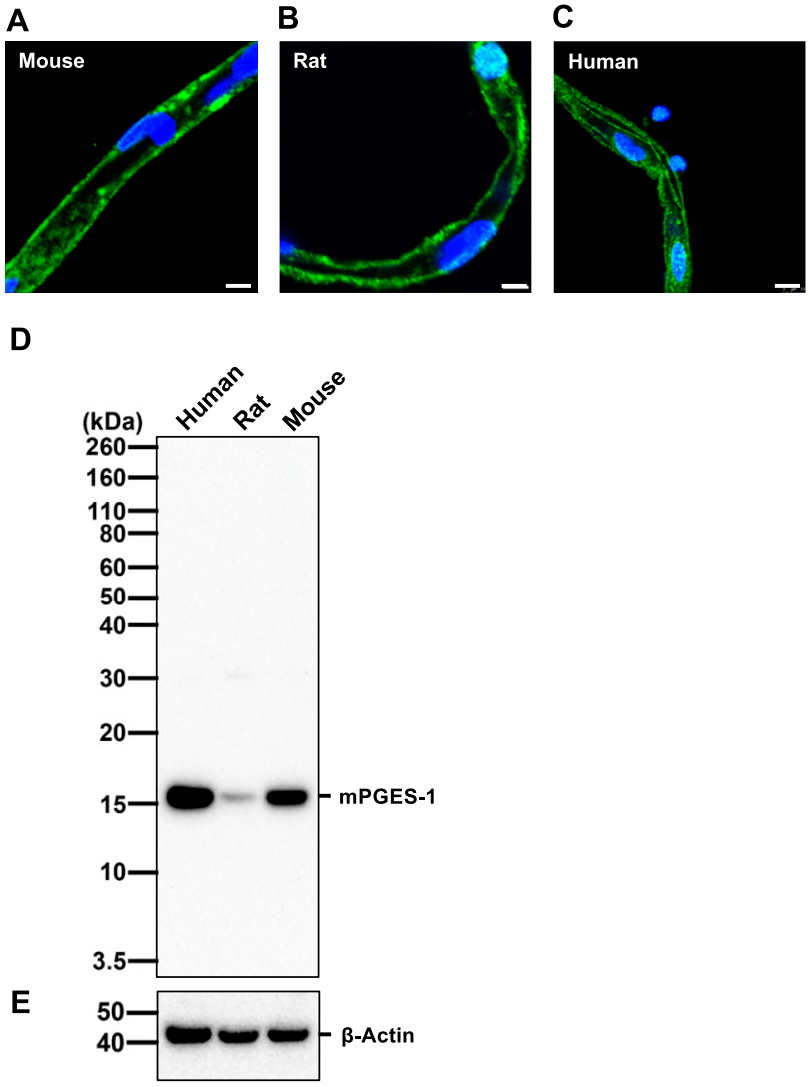

Figure 4. mPGES-1 protein expression in isolated mouse, rat, and human brain capillaries. *A–C*) Representative images of isolate moused (*A*), rat (*B*), and human (*C*) brain capillaries immunostained for mPGES-1 (green); nuclei are counterstained with DAPI (blue). Scale bar, 5 μm. *D*, *E*) Western blot showing hmPGES-1 protein expression (*D*) in isolated capillary membranes from mouse, rat and human brain tissue; β-actin was used as protein loading control (*E*).

BI1029539 blocks glutamate-mediated P-gp up-regulation *ex vivo*

To extend our findings to hmPGES-1, we used transgenic mice expressing hmPGES-1. We employed this unique humanized mPGES-1–expressing mouse model in combination with BI1029539, a potent and specific inhibitor for hmPGES-1 (26, 27). **Figure 5*A*** shows a representative image of an isolated capillary from hmPGES-1 mice immunostained for hmPGES-1 with an antibody that is specific for hmPGES-1 and does not react with mouse or rat mPGES-1. The negative control (no primary antibody) showed no staining for hmPGES-1 (Fig. 5*B*). Exposing isolated brain capillaries from hmPGES-1 mice to 100 μM glutamate increased P-gp protein expression levels; glutamate also slightly increased hmPGES-1 protein expression levels (Fig. 5*C*; for Western blot analyses see Table 3). In capillaries exposed to both glutamate and BI1029539, the glutamate effect on P-gp was blocked. As an additional control, we tested the effect of BI1029539 by itself, which did not affect P-gp protein levels. Consistent with glutamate-mediated induction of P-gp protein expression, P-gp transport activity was also increased with glutamate; BI1029539 completely abolished this effect. Figure 5*D* shows representative images of brain capillaries from hmPGES-1 mice after addition of NBD-CSA to determine P-gp transport activity. Compared with control capillaries, glutamate-treated capillaries showed increased luminal NBD-CSA fluorescence, indicating increased P-gp transport activity levels. In contrast, BI1029539 treatment maintained luminal NBD-CSA fluorescence at control levels; BI1029539 itself had no effect on luminal NBD-CSA fluorescence levels. Confocal image analysis revealed that in glutamate-treated brain capillaries, specific luminal NBD-CSA fluorescence was significantly increased by 73.2% ($P < 0.001$) (Fig. 5*E*). BI1029539 blocked the glutamate effect and P-gp transport activity remained at control levels; BI1029539 itself had no effect on P-gp transport activity.

Next, we conducted a dose response to determine the lowest concentration at which BI1029539 inhibits glutamate-induced P-gp up-regulation in brain capillaries. We exposed brain capillaries isolated from transgenic hmPGES-1 mice to glutamate in the presence of 1, 10, or 100 nM BI1029539. The Western blot in **Fig. 6*A*** (Western blot analyses in Table 4) shows that glutamate increased P-gp protein expression levels and that this effect was

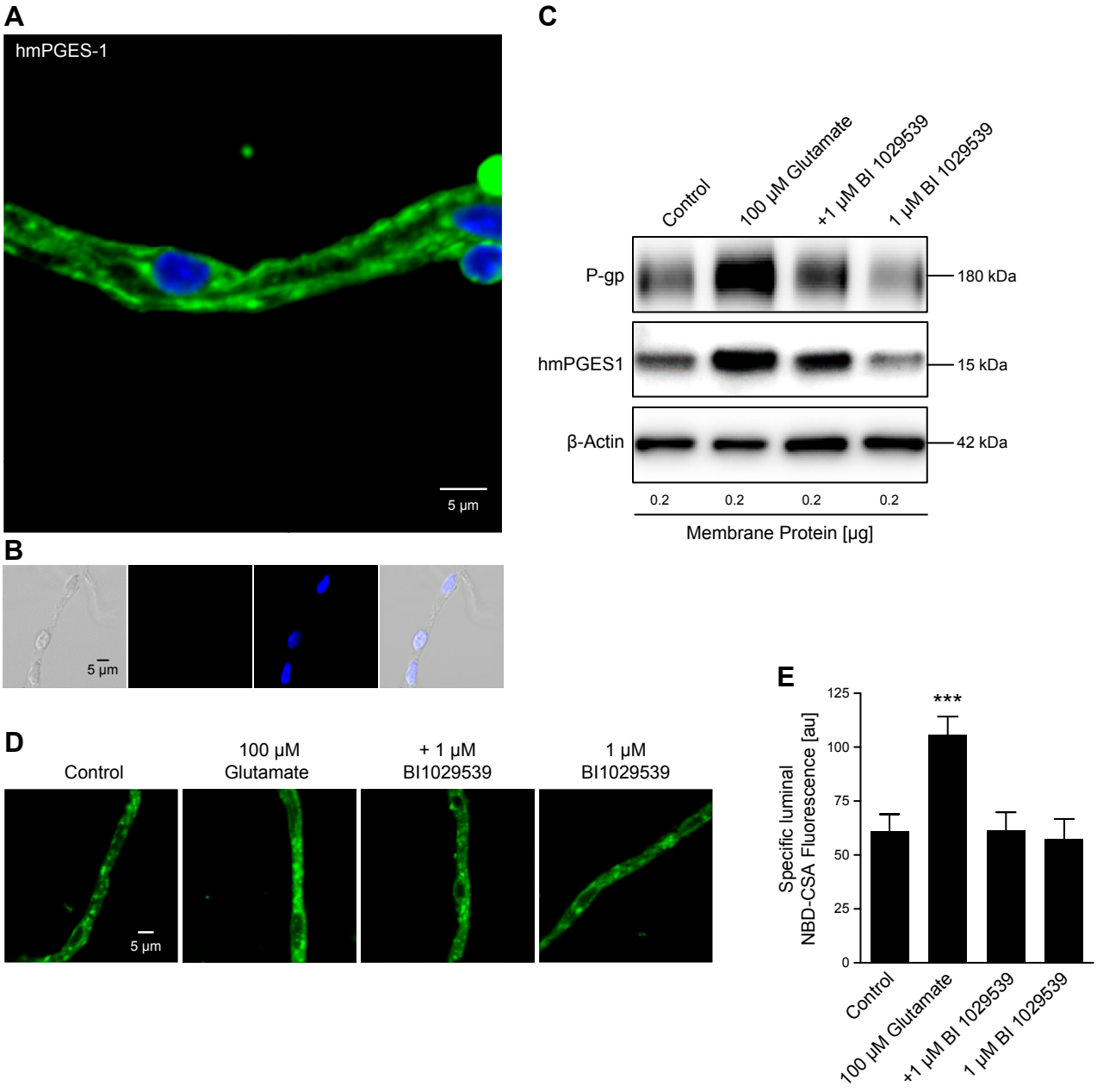

Figure 5. BI1029539 effect on glutamate-mediated up-regulation of P-gp and mPGES-1 levels in isolated brain capillaries. *A*) Isolated brain capillary from hmPGES-1 mice immunostained for hmPGES-1 (green); nuclei are counterstained with DAPI (blue). Scale bar, 5 µm. *B*) Negative control (no primary antibody) from left to right: transmitted light channel, green channel, blue channel, overlay of all 3 channels. Scale bar, 5 µm. *C*) Exposing isolated brain capillaries from hmPGES-1 mice to 100 µM glutamate increased P-gp protein expression levels. The glutamate effect on P-gp was blocked by 1 µM BI1029539, which by itself did not affect P-gp. Glutamate also slightly increased hmPGES1 protein levels in brain capillaries from hmPGES-1 mice; BI1029539 blocked this effect as well. BI1029539 itself did not affect hmPGES-1 protein levels. β-Actin was used as protein loading control. *D*) Representative images of brain capillaries from hmPGES-1 mice after addition of NBD-CSA to determine P-gp transport activity. Glutamate-treated capillaries show increased luminal NBD-CSA accumulation compared with controls. BI1029539 treatment maintained luminal NBD-CSA fluorescence at control levels; BI1029539 itself had no effect on luminal NBD-CSA fluorescence. Scale bar, 5 µm. *E*) Image analysis revealed that specific luminal NBD-CSA fluorescence was increased in glutamate-treated capillaries. BI1029539 blocked the glutamate effect and had no effect on P-gp transport activity by itself. For specific luminal NBD-CSA fluorescence, each data point represents means ± SEM for 10 capillaries from 1 preparation of 50 hmPGES-1 mice. Units are arbitrary units (au; scale: 0–255). $^{***}P < 0.001$, significantly higher than controls.

blocked by 1, 10, and 100 nM BI1029539. Glutamate also increased hmPGES-1 protein expression levels in brain capillaries. This effect was only blocked at higher BI1029539 concentrations of 10 and 100 nM.

Consistent with glutamate-mediated induction of P-gp protein expression, glutamate also increased P-gp transport activity, and this effect was abolished by BI1029539 at all concentrations used. Figure 6*B* shows representative

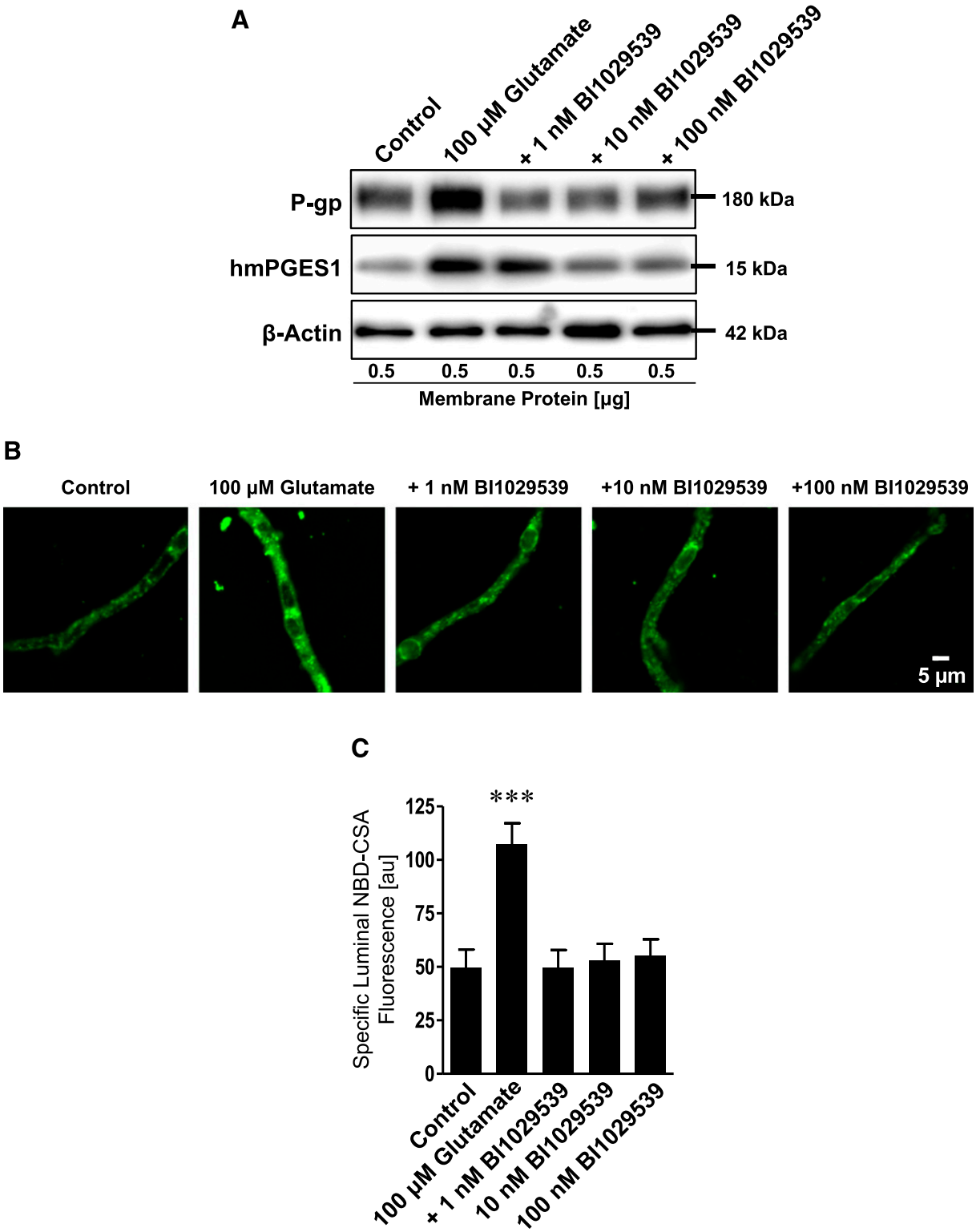

Figure 6. BI1029539 effect on glutamate-mediated up-regulation of P-gp and mPGES-1 levels in isolated brain capillaries *ex vivo*. *A*) P-gp and hmPGES-1 Western blot. Exposing brain capillaries from hmPGES-1 mice to 100 µM glutamate increased P-gp protein expression levels. The glutamate effect on P-gp was blocked by 1, 10, and 100 nM BI1029539. Glutamate also increased hmPGES-1 protein levels in brain capillaries from hmPGES-1 mice; 10 and 100 nM BI1029539 blocked this effect as well. β-Actin was used as protein loading control. *B*) Representative images of brain capillaries isolated from hmPGES-1 mice after addition of NBD-CSA to determine P-gp transport activity. Glutamate-treated capillaries show increased luminal NBD-CSA accumulation compared with controls. BI1029539 treatment maintained luminal NBD-CSA fluorescence at control levels. Scale bar, 5 µm. *C*) Image analysis revealed that specific luminal NBD-CSA fluorescence was increased in glutamate-treated capillaries. BI1029539 at all concentrations tested blocked the glutamate effect. For specific luminal NBD-CSA fluorescence, each data point represents means ± SEM for 10 capillaries from 1 preparation of 70 hmPGES-1 mice. Units are arbitrary units (au; scale: 0–255). ***$P <$ 0.001, significantly higher than controls.

images of brain capillaries from hmPGES-1 mice after exposure to glutamate and addition of NBD-CSA to determine P-gp transport activity. Compared with control capillaries, luminal NBD-CSA fluorescence was increased in glutamate-treated capillaries, indicating increased P-gp transport activity levels. In contrast, BI1029539 treatment maintained luminal NBD-CSA fluorescence at control levels. Quantitative confocal image analysis revealed that specific luminal NBD-CSA fluorescence was increased by 116.5% ($P < 0.001$) in brain capillaries treated with glutamate compared with control and that BI1029539 at 1, 10, and 100 nM blocked this glutamate effect on P-gp transport activity (Fig. 6*C*).

BI1029539 blocks SE-mediated up-regulation of P-gp expression and activity *in vivo*

To test the effect of BI1029539 inhibition of hmPGES-1 on P-gp *in vivo*, transgenic hmPGES-1 mice were treated with BI1029539. BI1029539 treatment included dosing mice by intraperitoneal injection 4 times prior to SE induction and 3 times after SE induction. Three groups of mice were treated with either 10, 30, or 100 mg/kg BI1029539. Forty-eight hours after SE, animals were euthanized, and brain capillaries were isolated for analysis. The Western blot in **Fig. 7*A*** (Western blot analyses in Table 5) shows that kainic acid–induced SE substantially increased P-gp protein expression levels in brain capillary membranes from hmPGES-1 mice compared with control hmPGES-1 mice that did not experience SE. The SE-induced increase in P-gp protein expression levels was blocked by 10, 30, and 100 mg/kg BI1029539. Kainic acid–induced SE in hmPGES-1 mice also slightly increased hmPGES-1 protein levels in brain capillaries, and this effect was blocked with 10, 30, and 100 mg/kg BI1029539 as well. An additional group of hmPGES-1 mice that were dosed with 100 mg/kg BI1029539 showed that BI1029539 by itself did not have any effect on P-gp or hmPGES-1 protein expression levels in brain capillaries *in vivo*. Consistent with increased P-gp protein expression levels, P-gp transport activity levels were increased in brain capillaries from hmPGES-1 mice after SE. Note that P-gp protein expression is also increased in capillaries from kainic acid control mice that experienced a few seizures but did not develop SE, suggesting a dose-response–like relation between seizures and P-gp protein expression levels (25).

Figure 7*B* shows representative confocal images of brain capillaries that were isolated from hmPGES-1 mice and exposed to NBD-CSA to determine P-gp transport activity. Compared with capillaries from control mice, luminal NBD-CSA fluorescence in brain capillaries from hmPGES-1 mice after SE was increased, indicating increased P-gp transport activity. In contrast, BI1029539 at 10, 30, and 100 mg/kg abolished this effect and maintained luminal NBD-CSA fluorescence at levels comparable to those observed in brain capillaries from control hmPGES-1 mice. Quantitative confocal image analysis showed that specific luminal NBD-CSA fluorescence was increased by 41% ($P < 0.001$) in brain capillaries from hmPGES-1 mice with kainic acid–induced SE compared with control (Fig. 7*C*), indicating increased P-gp transport activity levels. No such increase in P-gp transport activity was observed in brain capillaries isolated from animals treated with 10, 30, or 100 mg/kg BI1029539. In these animals, BI1029539 fully blocked the SE-induced increase in P-gp transport activity, which remained at levels comparable to those in brain capillaries from control hmPGES-1 mice. In brain capillaries from mice dosed with 100 mg/kg BI1029539, P-gp transport activity remained at levels similar to those in control animals, indicating that BI1029539 by itself did not have any effect on P-gp transport activity.

These data indicate that hmPGES-1 is involved in SE-induced up-regulation of P-gp protein expression and transport activity levels at the blood-brain barrier.

DISCUSSION

We have previously shown up-regulation of blood-brain barrier P-gp by glutamate through COX-2 and EP1 (9, 12, 20, 25). In the present study, we postulated that inhibiting mPGES-1, the enzyme responsible for PGE2 production, would block seizure-mediated up-regulation of P-gp protein expression and transport activity levels at the blood-brain barrier. In the following sections, we discuss our findings.

First, current literature indicates that extracellular glutamate released during seizures increases ictal activity and excitotoxicity, resulting in a potentiation of seizures. Moreover, seizure-induced glutamate release is also implicated in up-regulation of blood-brain barrier drug efflux transporters such as P-gp, thereby limiting brain ASD levels (7, 12, 25, 46, 47). Here we show that exposing isolated rat and mouse brain capillaries to glutamate, NMDA, AA, PGH2, or PGE2 increases P-gp protein expression and transport activity levels (Figs. 2, 3, 5, and 6). The effect glutamate, NMDA, AA, PGH2, or PGE2 has on P-gp levels was completely abolished by blocking EP1 with SC-51089 (Fig. 3). Using BI1029539 to inhibit hmPGES-1 activity abolished glutamate-induced up-regulation of P-gp expression and activity levels. These findings support our previous observations that P-gp up-regulation is mediated through COX-2 and EP1 and indicate that mPGES-1 is a critical part of this signaling pathway responsible for glutamate-mediated up-regulation of blood-brain barrier P-gp (9, 20).

Second, we observed that glutamate also increased endothelial mPGES-1 protein expression levels in brain capillaries (Figs. 5 and 6). Our data are consistent with the observation that endothelial hmPGES-1 protein expression levels and PGE2 levels are significantly increased in mice after SE (6). Increased PGE2 levels have also been observed in cultured hippocampal slices following exposure to exogenous glutamate and in mouse cortex following ischemic stroke, which is also characterized by glutamate excitotoxicity (23). We further demonstrate that the hmPGES-1 inhibitor BI1029539

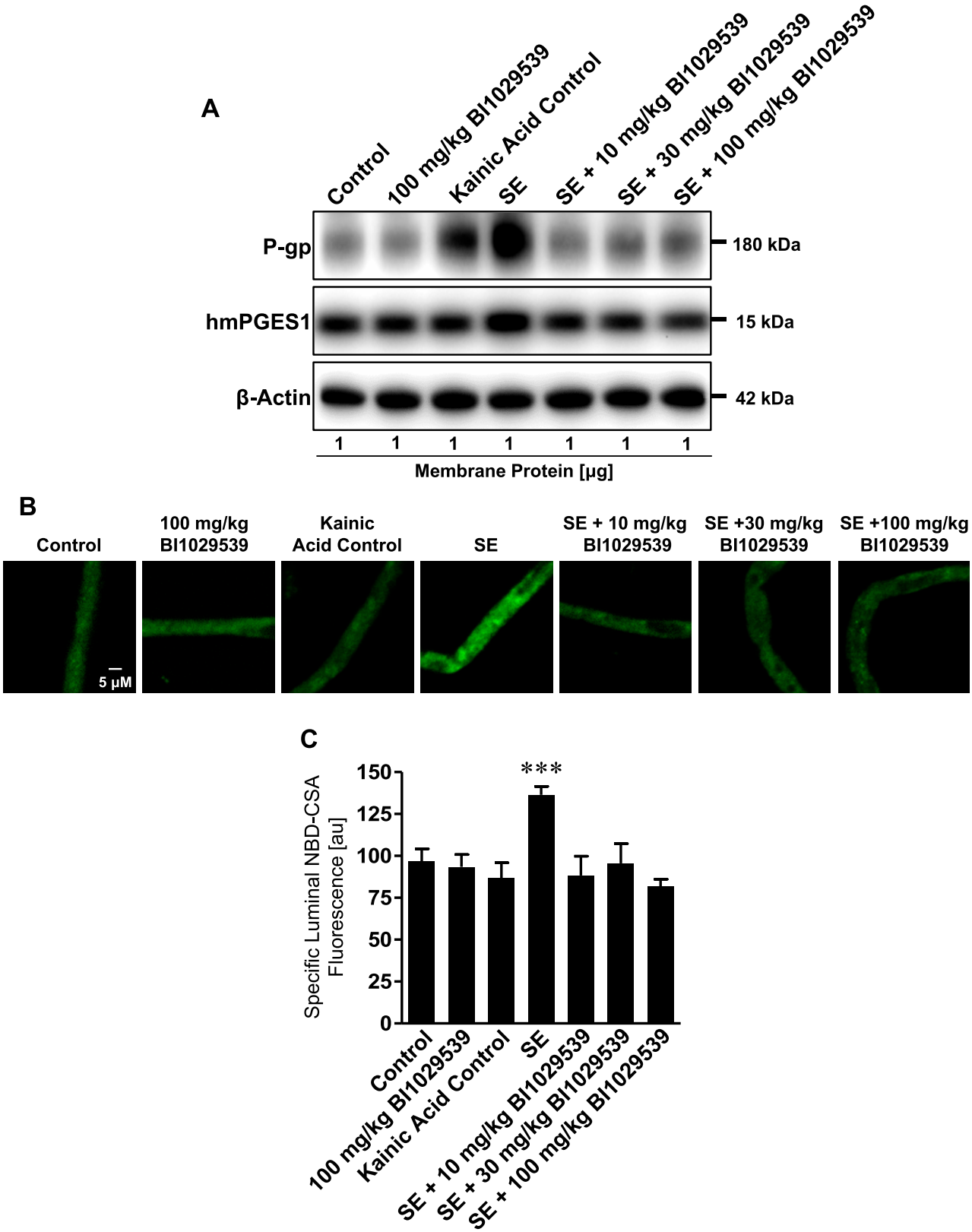

Figure 7. BI1029539 effect on seizure-induced up-regulation of P-gp and mPGES-1 levels *in vivo*. *A*) Western blot for P-gp and hmPGES-1 showing that kainic acid–induced SE increased P-gp protein expression levels in brain capillaries *in vivo*. This effect on P-gp was blocked by dosing hmPGES-1 mice with 10, 30, and 100 mg/kg BI1029539. SE also slightly increased hmPGES-1 protein levels in brain capillaries from hmPGES-1 mice; 10, 30, and 100 mg/kg BI1029539 blocked this effect as well. β-Actin was used as protein loading control. *B*) Representative images of brain capillaries isolated from hmPGES-1 mice after addition of NBD-CSA to determine P-gp transport function. Brain capillaries from mice that developed SE after kainic acid injection show increased luminal NBD-CSA accumulation compared with control mice. BI1029539 treatment blocked the SE effect and maintained

(*continued on next page*)

ablated glutamate-induced overexpression of endothelial hmPGES-1 (Figs. 5 and 6). Previous *in vitro* studies of human gingival fibroblasts and synovial fibroblasts showed a positive feedback between mPGES-1 expression and its product PGE2 (48, 49). Induction of mPGES-1 is known to occur in various cell types. Following SE, Takemiya *et al.* (6) immunostained brain slices and detected mPGES-1 protein expression in endothelial cells, but not in neurons or astrocytes. The researchers concluded that the brain endothelium is the largest source of PGE2 following seizures. Here, we show expression of mPGES-1 in isolated brain capillaries from mouse, rat, and human brain tissue (Fig. 4). Our mPGES-1 immunostaining data suggest that mPGES-1 is localized to the luminal and abluminal membranes. Data from a previous report [Takemiya *et al.* (6)] indicate that mPGES-1 colocalizes with COX-2 at the luminal endothelial membrane, suggesting that the 2 enzymes are functionally linked and that brain endothelial cells play an essential role in PGE2 production. The mPGES-1 Western blot data show substantially different expression levels between hmPGES-1 and mouse mPGES-1 *vs.* rat mPGES-1. The antibody we used was raised against mouse mPGES-1, but the epitope sequences of rat mPGES-1 and hmPGES-1 are 95 and 87%, respectively, of mouse mPGES-1. Thus, we conclude that the difference in expression levels is due not to antibody specificity between mouse, rat, and human but rather to species-specific basal mPGES-1 expression levels. This phenomenon has been observed before in a comparison of mPGES-1 protein expression levels in testicular tissue from rat, rabbit, pig, and monkey (50).

Third, conflicting reports exist in the literature on the effects of COX-2 inhibition on SE. Oliveira *et al.* (8) showed that inhibiting COX-2 potentiates pentylenetetrazol-induced SE, whereas data from Kelley *et al.* (51) show that transgenic mice overexpressing human COX-2 have reduced seizure thresholds when undergoing SE induction with kainic acid. In contrast, Takemiya *et al.* showed in COX-2 knockout mice a decreased susceptibility to electrical kindling compared with sham-treated control mice (52). These conflicting results have been attributed to the timing of inhibiting COX-2 relative to the time of seizure occurrence and the temporal profile of prostaglandin production (10, 53). Specifically, published results suggest a higher ratio of the anticonvulsant prostaglandin F2-α (PGF2-α) to the proconvulsant PGE2 during the SE onset phase compared with lower PGF2-α:PGE2 ratios during the SE progression and the late SE phases, indicating that PGE2 levels increase with SE progression (8, 10). In contrast, COX-2 activity predominates in nonneuronal cells after SE onset, at a time point when PGE2 predominates over PGF2-α (10, 54). van Vliet *et al.* (11) showed that inhibiting COX-2 in a rat model of chronic recurring seizures decreases brain PGE2 and leads to increased phenytoin brain: plasma ratios. Thus, these observations suggest that inhibiting COX-2 signaling could improve ASD brain delivery and ultimately reduce seizure burden. However, COX-2 inhibitors have considerable disadvantages because of their potential for severe side effects. In this regard, inhibition of mPGES-1 increases prostacyclin (PGI2) synthesis, which results in reduced vasoconstriction and lower cardiovascular side effects compared with COX-2 inhibitors (55). Therefore, targeting hmPGES-1 could be an alternative target to minimize adverse effects and maximize therapeutic benefits.

Fourth, up-regulation of blood-brain barrier P-gp in various animal SE models, including the kainic acid SE model, is well documented (17, 18, 22, 56). To investigate the effect of mPGES-1 inhibition on seizure-induced P-gp up-regulation, we dosed mice expressing hmPGES-1 with BI1029539. Only in BI1029539-untreated animals that experienced SE we observed increased P-gp expression and transport activity levels in brain capillaries. In BI1029539-untreated mice that were dosed with kainic acid but did not develop SE (kainic acid control animals), brain capillary P-gp protein expression levels were slightly elevated, but transport activity remained at control levels. It is noteworthy that hmPGES-1 inhibition with BI1029539 did not reduce, delay, or affect kainic acid–induced SE. This observation supports the idea of a dose response, in which animals that did not experience SE but still had a few seizures showed lower P-gp induction compared with animals that experienced SE (25). Importantly, BI1029539 at all dose levels effectively prevented the SE-induced increase of P-gp protein expression and transport activity levels. In control mice (no kainic acid), BI1029539 had no effect on basal P-gp protein expression and transport activity levels. In addition to P-gp expression and transport function, SE also induced endothelial hmPGES-1 expression in isolated brain microvessels, supporting observations made by Takemiya *et al.* (6) who showed mPGES-1 up-regulation following kainic acid–induced SE in mice. Consistent with our *ex vivo* observations that BI1029539 blocked glutamate-induced hmPGES-1 overexpression, inhibiting hmPGES-1 with BI1029539 prevented SE-induced overexpression of hmPGES-1 *in vivo*. This suggests that the positive feedback between mPGES-1 and PGE2 observed *in vitro* also occurs following seizures *in vivo* (48, 49). Given the effect of hmPGES-1 inhibition on P-gp expression and transport activity after SE, we conclude that mPGES-1 is a critical

luminal NBD-CSA fluorescence at control levels. Scale bar, 5 μm. *C*) Image analysis showed that specific luminal NBD-CSA fluorescence was increased in capillaries from SE animals indicating increased P-gp transport activity. No such increase was found in capillaries from SE animals that received BI1029539. For specific luminal NBD-CSA fluorescence, each data point represents the mean ± SEM for 10 capillaries from pooled brain tissue of all mice per group (control $n = 20$, 100 mg/kg BI1029539 $n = 20$, kainic acid control $n = 12$, SE $n = 16$, SE + 10 mg/kg BI1029539 $n = 20$, SE + 30 mg/kg BI1029539 $n = 17$, SE + 100 mg/kg BI1029539 $n = 22$). Units are arbitrary units (au; scale: 0–255). $^{***}P < 0.001$, significantly higher than controls.

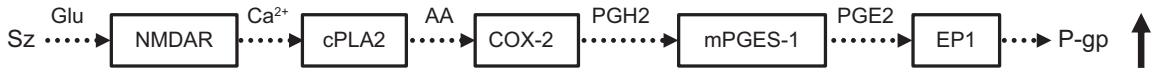

Figure 8. Proposed signaling pathway in brain capillaries. Based on our data presented here and our previously published data, we propose that seizure-induced (Sz) release of glutamate signals through the NMDA receptor (NMDAR), which leads to activation of cPLA2. This, in turn, leads to release of AA, which COX-2 converts to PGH2. mPGES-1 converts PGH2 to PGE2, which signals through EP1, leading to increased P-gp protein expression and transport activity levels at the blood-brain barrier.

component in the signaling pathway that modulates blood-brain barrier P-gp during and after seizures.

In accordance with our previous studies, the data presented here demonstrate that inhibiting hmPGES-1 and EP-1 prevents SE-induced up-regulation of P-gp expression and transport activity. These findings support our postulated signaling pathway (**Fig. 8**). Based on our present and previously published data, we propose that seizure-released glutamate signals through the NMDA receptor to activate $cPLA_2$, leading to an increase in production of AA, which is converted by COX-2–mPGES-1 into PGE2. Increased PGE2 levels lead to activation of the endothelial EP1 receptor, which results in P-gp up-regulation (9, 12, 20). Although our present data show that hmPGES-1 inhibition with BI1029539 abolishes SE- and glutamate-induced up-regulation of P-gp protein expression and transport function in brain capillaries, we currently do not know if BI1029539 causes pathway shift, *i.e.*, reduces PGE2 synthesis or changes levels of other prostanoids. It is possible that inhibition of mPGES-1 leads to PGI2 production through PGI2 synthase.

Fifth, although mPGES-1 inhibition itself does not prevent SE development, it is important to determine mPGES-1 inhibition efficacy with regard to reducing seizure burden and ASD distribution in a chronic epilepsy model. Several studies have provided evidence that PGE2 maintains SE and plays a role in epilepsy (6–8, 10, 11, 15, 53). Given that: *1*) PGE2 levels are increased in SE, that *2*) PGE2 is involved in P-gp up-regulation after seizures, and that *3*) PGE2 contributes to ictal activity and excitotoxicity, mPGES-1 could be a promising target to reduce P-gp expression and transport activity levels, which would be expected to lead to increased ASD brain levels, and thus reduce seizure burden in ASD-resistant epilepsy (9, 10, 20, 46, 47, 54).

Finally, in this study we demonstrate that inhibiting hmPGES-1 with BI1029539 effectively prevents glutamate-mediated induction of P-gp protein expression and transport activity in isolated mouse brain capillaries *ex vivo* and in brain capillaries of a mouse SE model *in vivo*. Inhibiting hmPGES-1 also prevented hmPGES-1 induction. Further studies are necessary to determine if mPGES-1 inhibition reduces PGE2 levels during SE and leads to increased ASD brain levels. Although susceptibility to kainic acid–induced SE was not reduced, mPGES-1 inhibition may still have a therapeutic benefit on reducing seizure burden by reducing blood-brain barrier P-gp expression and transport activity levels and by preventing seizure-induced mPGES-1 up-regulation. Further studies are required to determine if mPGES-1 inhibition during or after SE will reduce ASD resistance by improving ASD delivery into the brain and thus could potentially serve as a beneficial add-on treatment for epilepsy pharmacotherapy. FJ

ACKNOWLEDGMENTS

The authors thank members of the B.B. and A.M.S.H. laboratories for proofreading the manuscript. The authors acknowledge Dr. Marion Bankstahl and Dr. Wolfgang Löscher (both from the University of Veterinary Medicine Hannover, Hannover, Germany) for help with the kainic acid mouse status epilepticus model. This project was supported by funding from Boehringer Ingelheim Pharma (Biberach, Germany), and by U.S. National Institutes of Health (NIH) National Institute of Neurological Disorders and Stroke (NINDS) Grant 1R01NS079507 (to B.B.). The content is solely the responsibility of the authors and does not necessarily represent the official views of the NINDS or the NIH. The authors declare no conflicts of interest.

AUTHOR CONTRIBUTIONS

E. L. B. Soldner contributed to data acquisition and data analysis and drafted parts of the first version of the article; A. M. S. Hartz contributed to data acquisition, data analysis, and interpretation of data and drafted and revised the article; S.-I. Akanuma contributed to data acquisition, data analysis, and interpretation of data and drafted and revised the article; A. Pekcec contributed to interpretation of data and revised the article; H. Doods contributed to interpretation of data and revised the article; R. J. Kryscio contributed to data analysis (biostatistics) and drafted and revised the article; K.-I. Hosoya contributed to interpretation of data and revised the article; and B. Bauer contributed to data acquisition, data analysis, and interpretation of data and drafted and revised the article.

REFERENCES

1. Ngugi, A. K., Kariuki, S. M., Bottomley, C., Kleinschmidt, I., Sander, J. W., and Newton, C. R. (2011) Incidence of epilepsy: a systematic review and meta-analysis. *Neurology* **77**, 1005–1012
2. Tang, F., Hartz, A. M. S., and Bauer, B. (2017) Drug-resistant epilepsy: multiple hypotheses, few answers. *Front. Neurol.* **8**, 301
3. Guan, Y., Zhang, Y., Schneider, A., Riendeau, D., Mancini, J. A., Davis, L., Komhoff, M., Breyer, R. M., and Breyer, M. D. (2001) Urogenital distribution of a mouse membrane-associated prostaglandin E(2) synthase. *Am. J. Physiol. Renal Physiol.* **281**, F1173–F1177
4. Kobayashi, T., and Narumiya, S. (2002) Function of prostanoid receptors: studies on knockout mice. *Prostaglandins Other Lipid Mediat.* **68-69**, 557–573
5. Navarro, E., Romero, S. D., and Yaksh, T. L. (1989) CNS stimulation and PGE2 release. III. Pentamethylenetetrazole-induced seizures. *J. Cereb. Blood Flow Metab.* **9**, 180–186

6. Takemiya, T., Matsumura, K., Sugiura, H., Maehara, M., Yasuda, S., Uematsu, S., Akira, S., and Yamagata, K. (2010) Endothelial microsomal prostaglandin E synthase-1 exacerbates neuronal loss induced by kainate. *J. Neurosci. Res.* **88**, 381–390
7. Takemiya, T., Matsumura, K., Sugiura, H., Yasuda, S., Uematsu, S., Akira, S., and Yamagata, K. (2011) Endothelial microsomal prostaglandin E synthase-1 facilitates neurotoxicity by elevating astrocytic Ca2+ levels. *Neurochem. Int.* **58**, 489–496
8. Oliveira, M. S., Furian, A. F., Royes, L. F., Fighera, M. R., Fiorenza, N. G., Castelli, M., Machado, P., Bohrer, D., Veiga, M., Ferreira, J., Cavalheiro, E. A., and Mello, C. F. (2008) Cyclooxygenase-2/PGE2 pathway facilitates pentylenetetrazol-induced seizures. *Epilepsy Res.* **79**, 14–21
9. Pekcec, A., Unkruer, B., Schlichtiger, J., Soerensen, J., Hartz, A. M., Bauer, B., van Vliet, E. A., Gorter, J. A., and Potschka, H. (2009) Targeting prostaglandin E2 EP1 receptors prevents seizure-associated P-glycoprotein up-regulation. *J. Pharmacol. Exp. Ther.* **330**, 939–947
10. Takemiya, T., Maehara, M., Matsumura, K., Yasuda, S., Sugiura, H., and Yamagata, K. (2006) Prostaglandin E2 produced by late induced COX-2 stimulates hippocampal neuron loss after seizure in the CA3 region. *Neurosci. Res.* **56**, 103–110
11. van Vliet, E. A., Zibell, G., Pekcec, A., Schlichtiger, J., Edelbroek, P. M., Holtman, L., Aronica, E., Gorter, J. A., and Potschka, H. (2010) COX-2 inhibition controls P-glycoprotein expression and promotes brain delivery of phenytoin in chronic epileptic rats. *Neuropharmacology* **58**, 404–412
12. Bauer, B., Hartz, A. M., Pekcec, A., Toellner, K., Miller, D. S., and Potschka, H. (2008) Seizure-induced up-regulation of P-glycoprotein at the blood-brain barrier through glutamate and cyclooxygenase-2 signaling. *Mol. Pharmacol.* **73**, 1444–1453
13. Brandt, C., Bethmann, K., Gastens, A. M., and Loscher, W. (2006) The multidrug transporter hypothesis of drug resistance in epilepsy: Proof-of-principle in a rat model of temporal lobe epilepsy. *Neurobiol. Dis.* **24**, 202–211
14. Luna-Tortós, C., Fedrowitz, M., and Löscher, W. (2008) Several major antiepileptic drugs are substrates for human P-glycoprotein. *Neuropharmacology* **55**, 1364–1375
15. Löscher, W., and Schmidt, D. (2002) New horizons in the development of antiepileptic drugs. *Epilepsy Res.* **50**, 3–16
16. Pekcec, A., Unkruer, B., Stein, V., Bankstahl, J. P., Soerensen, J., Tipold, A., Baumgartner, W., and Potschka, H. (2009) Over-expression of P-glycoprotein in the canine brain following spontaneous status epilepticus. *Epilepsy Res.* **83**, 144–151
17. Rizzi, M., Caccia, S., Guiso, G., Richichi, C., Gorter, J. A., Aronica, E., Aliprandi, M., Bagnati, R., Fanelli, R., D'Incalci, M., Samanin, R., and Vezzani, A. (2002) Limbic seizures induce P-glycoprotein in rodent brain: functional implications for pharmacoresistance. *J. Neurosci.* **22**, 5833–5839
18. Seegers, U., Potschka, H., and Loscher, W. (2002) Expression of the multidrug transporter P-glycoprotein in brain capillary endothelial cells and brain parenchyma of amygdala-kindled rats. *Epilepsia* **43**, 675–684
19. Tishler, D. M., Weinberg, K. I., Hinton, D. R., Barbaro, N., Annett, G. M., and Raffel, C. (1995) MDR1 gene expression in brain of patients with medically intractable epilepsy. *Epilepsia* **36**, 1–6
20. Zibell, G., Unkruer, B., Pekcec, A., Hartz, A. M., Bauer, B., Miller, D. S., and Potschka, H. (2009) Prevention of seizure-induced up-regulation of endothelial P-glycoprotein by COX-2 inhibition. *Neuropharmacology* **56**, 849–855
21. Schlichtiger, J., Pekcec, A., Bartmann, H., Winter, P., Fuest, C., Soerensen, J., and Potschka, H. (2010) Celecoxib treatment restores pharmacosensitivity in a rat model of pharmacoresistant epilepsy. *Br. J. Pharmacol.* **160**, 1062–1071
22. Volk, H. A., and Loscher, W. (2005) Multidrug resistance in epilepsy: rats with drug-resistant seizures exhibit enhanced brain expression of P-glycoprotein compared with rats with drug-responsive seizures. *Brain* **128**, 1358–1368
23. Ikeda-Matsuo, Y., Hirayama, Y., Ota, A., Uematsu, S., Akira, S., and Sasaki, Y. (2010) Microsomal prostaglandin E synthase-1 and cyclooxygenase-2 are both required for ischaemic excitotoxicity. *Br. J. Pharmacol.* **159**, 1174–1186
24. Curtis, M. J., Bond, R. A., Spina, D., Ahluwalia, A., Alexander, S. P., Giembycz, M. A., Gilchrist, A., Hoyer, D., Insel, P. A., Izzo, A. A., Lawrence, A. J., MacEwan, D. J., Moon, L. D., Wonnacott, S., Weston, A. H., and McGrath, J. C. (2015) Experimental design and analysis and their reporting: new guidance for publication in BJP. *Br. J. Pharmacol.* **172**, 3461–3471
25. Hartz, A. M., Pekcec, A., Soldner, E. L., Zhong, Y., Schlichtiger, J., and Bauer, B. (2017) P-gp protein expression and transport activity in rodent seizure models and human epilepsy. *Mol. Pharm.* **14**, 999–1011
26. Gurusamy, M. N. A., Ambade, H., Lee, H., Pekcec, A., Doods, H., and Wu, D. (2016) Inhibition of mPGES-1 reduces acute lung injury in mice. *Respirology* **21**, APSR6-0278 (abstr.)
27. Priepke, H., Doods, H., Kuelzer, R., Pfau, R., Stenkamp, D., Pelcman, B., Roenn, R., Lubriks, D., Suna, E., inventors; Boehringer Ingelheim International GmBH, assignee. (2012) 2-(Arylamino)-3H-imidazo [4,5-B]pyridine-6-carboxamide derivatives and their use as mPGES-1 inhibitors [patent]. World Intellectual Property Organization (WIPO) Patentscope no. WO2012022792. February 23, 2012
28. Akanuma, S.-I., Higuchi, T., Higashi, H., Ozeki, G., Tachikawa, M., Kubo, Y., and Hosoya, K. (2014) Transporter-mediated prostaglandin E(2) elimination across the rat blood-brain barrier and its attenuation by the activation of N-methyl-D-aspartate receptors. *Drug Metab. Pharmacokinet.* **29**, 387–393
29. Eskilsson, A., Tachikawa, M., Hosoya, K., and Blomqvist, A. (2014) Distribution of microsomal prostaglandin E synthase-1 in the mouse brain. *J. Comp. Neurol.* **522**, 3229–3244
30. Tachikawa, M., Ozeki, G., Higuchi, T., Akanuma, S.-I., Tsuji, K., and Hosoya, K. (2012) Role of the blood-cerebrospinal fluid barrier transporter as a cerebral clearance system for prostaglandin E(2) produced in the brain. *J. Neurochem.* **123**, 750–760
31. Schramm, U., Fricker, G., Wenger, R., and Miller, D. S. (1995) P-glycoprotein-mediated secretion of a fluorescent cyclosporin analogue by teleost renal proximal tubules. *Am. J. Physiol.* **268**, F46–F52
32. Xu, D., Rowland, S. E., Clark, P., Giroux, A., Cote, B., Guiral, S., Salem, M., Ducharme, Y., Friesen, R. W., Methot, N., Mancini, J., Audoly, L., and Riendeau, D. (2008) MF63 [2-(6-chloro-1H-phenanthro[9,10-d] imidazol-2-yl)-isophthalonitrile], a selective microsomal prostaglandin E synthase-1 inhibitor, relieves pyresis and pain in preclinical models of inflammation. *J. Pharmacol. Exp. Ther.* **326**, 754–763
33. Nelson, P. T., Jicha, G. A., Schmitt, F. A., Liu, H., Davis, D. G., Mendiondo, M. S., Abner, E. L., and Markesbery, W. R. (2007) Clinicopathologic correlations in a large Alzheimer disease center autopsy cohort: neuritic plaques and neurofibrillary tangles "do count" when staging disease severity. *J. Neuropathol. Exp. Neurol.* **66**, 1136–1146
34. Hellier, J. L., and Dudek, F. E. (2005) Chemoconvulsant model of chronic spontaneous seizures. *Curr. Protoc. Neurosci.* **Chapter 9**, Unit 9.19
35. Bauer, B., Hartz, A. M., and Miller, D. S. (2007) Tumor necrosis factor alpha and endothelin-1 increase P-glycoprotein expression and transport activity at the blood-brain barrier. *Mol. Pharmacol.* **71**, 667–675
36. Hartz, A. M., Bauer, B., Fricker, G., and Miller, D. S. (2006) Rapid modulation of P-glycoprotein-mediated transport at the blood-brain barrier by tumor necrosis factor-alpha and lipopolysaccharide. *Mol. Pharmacol.* **69**, 462–470
37. Bauer, B., Hartz, A. M., Fricker, G., and Miller, D. S. (2004) Pregnane X receptor up-regulation of P-glycoprotein expression and transport function at the blood-brain barrier. *Mol. Pharmacol.* **66**, 413–419
38. Hartz, A. M., Bauer, B., Fricker, G., and Miller, D. S. (2004) Rapid regulation of P-glycoprotein at the blood-brain barrier by endothelin-1. *Mol. Pharmacol.* **66**, 387–394
39. Hartz, A. M., Bauer, B., Block, M. L., Hong, J. S., and Miller, D. S. (2008) Diesel exhaust particles induce oxidative stress, proinflammatory signaling, and P-glycoprotein up-regulation at the blood-brain barrier. *FASEB J.* **22**, 2723–2733
40. Hartz, A. M., Miller, D. S., and Bauer, B. (2010) Restoring blood-brain barrier P-glycoprotein reduces brain amyloid-beta in a mouse model of Alzheimer's disease. *Mol. Pharmacol.* **77**, 715–723
41. Samuelsson, B., Morgenstern, R., and Jakobsson, P. J. (2007) Membrane prostaglandin E synthase-1: a novel therapeutic target. *Pharmacol. Rev.* **59**, 207–224
42. Chen, S. H., Sung, Y. F., Oyarzabal, E. A., Tan, Y. M., Leonard, J., Guo, M., Li, S., Wang, Q., Chu, C. H., Chen, S. L., Lu, R. B., and Hong, J. S. (2018) Physiological concentration of prostaglandin E2 exerts anti-inflammatory effects by inhibiting microglial production of superoxide through a novel pathway. *Mol. Neurobiol.* **55**, 8001–8013
43. Minghetti, L., Greco, A., Cardone, F., Puopolo, M., Ladogana, A., Almonti, S., Cunningham, C., Perry, V. H., Pocchiari, M., and Levi, G. (2000) Increased brain synthesis of prostaglandin E2 and F2-isoprostane in human and experimental transmissible spongiform encephalopathies. *J. Neuropathol. Exp. Neurol.* **59**, 866–871

44. Minghetti, L., and Levi, G. (1998) Microglia as effector cells in brain damage and repair: focus on prostanoids and nitric oxide. *Prog. Neurobiol.* **54**, 99–125
45. Jakobsson, P. J., Thoren, S., Morgenstern, R., and Samuelsson, B. (1999) Identification of human prostaglandin E synthase: a microsomal, glutathione-dependent, inducible enzyme, constituting a potential novel drug target. *Proc. Natl. Acad. Sci. USA* **96**, 7220–7225
46. Ding, L., Wilke, C., Xu, B., Xu, X., van Drongelen, W., Kohrman, M., and He, B. (2007) EEG source imaging: correlating source locations and extents with electrocorticography and surgical resections in epilepsy patients. *J. Clin. Neurophysiol.* **24**, 130–136
47. Fellin, T., Gomez-Gonzalo, M., Gobbo, S., Carmignoto, G., and Haydon, P. G. (2006) Astrocytic glutamate is not necessary for the generation of epileptiform neuronal activity in hippocampal slices. *J. Neurosci.* **26**, 9312–9322
48. Kojima, F., Naraba, H., Sasaki, Y., Beppu, M., Aoki, H., and Kawai, S. (2003) Prostaglandin E2 is an enhancer of interleukin-1beta-induced expression of membrane-associated prostaglandin E synthase in rheumatoid synovial fibroblasts. *Arthritis Rheum.* **48**, 2819–2828
49. Yucel-Lindberg, T., Olsson, T., and Kawakami, T. (2006) Signal pathways involved in the regulation of prostaglandin E synthase-1 in human gingival fibroblasts. *Cell. Signal.* **18**, 2131–2142
50. Lazarus, M., Eguchi, N., Matsumoto, S., Nagata, N., Yano, T., Killian, G. J., and Urade, Y. (2004) Species-specific expression of microsomal prostaglandin E synthase-1 and cyclooxygenases in male monkey reproductive organs. *Prostaglandins Leukot. Essent. Fatty Acids* **71**, 233–240
51. Kelley, K. A., Ho, L., Winger, D., Freire-Moar, J., Borelli, C. B., Aisen, P. S., and Pasinetti, G. M. (1999) Potentiation of excitotoxicity in transgenic mice overexpressing neuronal cyclooxygenase-2. *Am. J. Pathol.* **155**, 995–1004
52. Takemiya, T., Suzuki, K., Sugiura, H., Yasuda, S., Yamagata, K., Kawakami, Y., and Maru, E. (2003) Inducible brain COX-2 facilitates the recurrence of hippocampal seizures in mouse rapid kindling. *Prostaglandins Other Lipid Mediat.* **71**, 205–216
53. Vezzani, A., and Granata, T. (2005) Brain inflammation in epilepsy: experimental and clinical evidence. *Epilepsia* **46**, 1724–1743
54. Desjardins, P., Sauvageau, A., Bouthillier, A., Navarro, D., Hazell, A. S., Rose, C., and Butterworth, R. F. (2003) Induction of astrocytic cyclooxygenase-2 in epileptic patients with hippocampal sclerosis. *Neurochem. Int.* **42**, 299–303
55. Ozen, G., Gomez, I., Daci, A., Deschildre, C., Boubaya, L., Teskin, O., Uydes-Dogan, B. S., Jakobsson, P. J., Longrois, D., Topal, G., and Norel, X. (2017) Inhibition of microsomal PGE synthase-1 reduces human vascular tone by increasing PGI2: a safer alternative to COX-2 inhibition. *Br. J. Pharmacol.* **174**, 4087–4098
56. Volk, H. A., Potschka, H., and Loscher, W. (2004) Increased expression of the multidrug transporter P-glycoprotein in limbic brain regions after amygdala-kindled seizures in rats. *Epilepsy Res.* **58**, 67–79

Received for publication June 12, 2019.
Accepted for publication September 10, 2019.